

**Spin dynamics in electron-doped iron pnictide superconductors**Yi Gao,<sup>1</sup> Tao Zhou,<sup>1,2</sup> C. S. Ting,<sup>1,3</sup> and Wu-Pei Su<sup>1</sup><sup>1</sup>*Department of Physics and Texas Center for Superconductivity, University of Houston, Houston, Texas 77204, USA*<sup>2</sup>*Department of Physics, Nanjing University of Aeronautics and Astronautics, Nanjing 210016, China*<sup>3</sup>*Department of Physics and Surface Physics Laboratory, Fudan University, Shanghai 200433, China*

(Received 21 June 2010; published 23 September 2010)

The doping dependence of spin excitations in  $\text{Ba}(\text{Fe}_{1-x}\text{Co}_x)_2\text{As}_2$  is studied based on a phenomenological two-orbital model under the random-phase approximation. We adopt this model because of its ability to fit the doping evolution of the Fermi surfaces and the asymmetry in the superconductivity (SC) coherent peaks as observed, respectively, by the angle-resolved photoemission spectroscopy (ARPES) and the scanning tunneling microscopy experiments in this type of compounds. The interplay between the spin-density wave and SC is considered in our calculation. Our results for the spin susceptibility are in qualitative agreement with neutron-scattering (NS) experiments in various doping ranges at temperatures above and below the superconducting transition temperature  $T_c$ . For the overdoped sample where one of the two hole pockets around  $\Gamma$  point disappears according to ARPES, we show that the imaginary part of the spin susceptibility in both SC and normal phases exhibits a gaplike behavior. This feature is consistent with the “pseudogap” as observed by recent nuclear magnetic resonance and NS experiments.

DOI: [10.1103/PhysRevB.82.104520](https://doi.org/10.1103/PhysRevB.82.104520)

PACS number(s): 74.70.Xa, 74.25.Ha, 75.30.Ds

**I. INTRODUCTION**

The recent discovery of the iron arsenide superconductors,<sup>1</sup> whose parent compounds exhibit long-range antiferromagnetic (AF) or spin-density-wave (SDW) order similar to the cuprates,<sup>2</sup> provides another promising group of materials for studying the interplay between magnetism and superconductivity (SC). Especially, the electron-doped pnictide superconductors such as  $\text{Ba}(\text{Fe}_{1-x}\text{Co}_x)_2\text{As}_2$  (Ref. 3) has been emerged as one of the most important systems due to the availability of large homogeneous single crystals. The phase diagram<sup>4–6</sup> for these materials indicates that the parent compound upon cooling through  $T_N \sim 140$  K (Ref. 7) develops a static SDW order. Increasing the doping of Co, the SDW order is suppressed and the SC order emerges as the temperature ( $T$ ) falls below  $T_c$ . The SDW and SC orders coexist in the underdoped samples.<sup>4–6,8</sup> By further increasing the Co concentration to the optimally doped regime, the SDW order disappears. These experimental results provide compelling evidences for strong competition between the SDW and SC orders.

Recently, several neutron-scattering (NS) experiments have been carried out to probe the spin dynamics in these materials,<sup>4–6,8–15</sup> and the spin excitation spectrum was fitted by using a  $J_1, J_2$  Heisenberg model based on localized spins.<sup>8,9,15,16</sup> However while the parent compounds of the cuprates are Mott insulators with large in-plane exchange interactions,<sup>17</sup> the parent iron arsenides are bad metals and remain itinerant at all doping levels. Magnetism in these materials are most likely to originate from itinerant electrons and the AF order is a result of SDW instability due to Fermi-surface nesting.<sup>18</sup> Theoretically, at present, the variation in the spin susceptibility with doping remains less explored. The spin susceptibilities were mostly studied in the optimally doped compounds without SDW (Ref. 19) or in the parent compound without SC,<sup>20</sup> as well as in the normal state with neither SDW nor SC.<sup>21</sup>

Another key issue here is the superconducting pairing symmetry. Experimental results about the pairing symmetry remain highly controversial, leaving the perspectives ranging from nodeless<sup>22,23</sup> to nodal gap structure.<sup>24–26</sup> Although evidence for a nodal gap has been accumulated in  $\text{LaFePO}$  (Ref. 25) and  $\text{Ba}(\text{FeAs}_{1-x}\text{P}_x)_2$  systems,<sup>26</sup> in the Co- and K-doped 122 family of iron pnictides, the experimental data points to the existence of isotropic gaps, especially in the optimally doped samples.<sup>23</sup> Theoretically it was suggested that the pairing may be established via inter-pocket scattering of electrons between the hole pockets (around the  $\Gamma$  point) and electron pockets (around the M point), leading to the so-called extended  $s$ -wave pairing symmetry ( $\Delta_{\mathbf{k}} \sim \cos k_x + \cos k_y$ ).<sup>18,27</sup>

In this work, we adopt Fermi-liquid mean-field (MF) theory to study the static SDW and SC, and employ the random-phase approximation (RPA) to investigate the spin dynamics in  $\text{Ba}(\text{Fe}_{1-x}\text{Co}_x)_2\text{As}_2$  from the imaginary part of the dynamic spin susceptibility. The SC order here is chosen to have extended  $s$ -wave symmetry which is supported by some theoretical studies<sup>18,27</sup> and experimental observations.<sup>23</sup> We show that the calculated spin susceptibilities are in qualitative agreement with several NS and nuclear magnetic resonance (NMR) experiments in various doping ranges, suggesting that in the 122 family of iron pnictides, the spin excitations can be qualitatively explained within the itinerant model.

**II. METHODOLOGY**

We start with a two-orbital model by taking into account two Fe ions per unit cell.<sup>28</sup> The validity of this model is controversial<sup>29,30</sup> since it lacks certain point-group symmetries for this compound as required by other band-structure calculations.<sup>31,32</sup> However, within our itinerant model, the spin dynamics are primarily determined by the Fermi-surface nesting condition and doping evolution, any tight-binding scheme with the similar Fermi-surface evolution should give

the similar results. In this regard, we adopt the model in Ref. 28 simply because of its ability<sup>33</sup> to qualitatively account for the doping evolution of the Fermi surface and the asymmetry in the SC coherent peaks as observed, respectively, by the angle-resolved photoemission spectroscopy (ARPES) (Ref. 34) and the scanning tunneling microscopy<sup>35</sup> experiments in Ba(Fe<sub>1-x</sub>Co<sub>x</sub>)<sub>2</sub>As<sub>2</sub>.

The Hamiltonian of our system can be expressed as<sup>33</sup>

$$H = H_0 + H_\Delta + H_{int}. \quad (1)$$

$H_0$  is the tight-binding Hamiltonian and can be written as<sup>28,33</sup>

$$H_0 = \sum_{\mathbf{k}\sigma} \psi_{\mathbf{k}\sigma}^\dagger M_{\mathbf{k}} \psi_{\mathbf{k}\sigma}, \quad (2)$$

where  $\psi_{\mathbf{k}\sigma}^\dagger = (c_{A0,\mathbf{k}\sigma}^\dagger, c_{A1,\mathbf{k}\sigma}^\dagger, c_{B0,\mathbf{k}\sigma}^\dagger, c_{B1,\mathbf{k}\sigma}^\dagger)$  is the creation operator with spin  $\sigma = -1$  ( $\downarrow$ ) or  $1$  ( $\uparrow$ ), in the orbitals  $(0, 1) = (d_{xz}, d_{yz})$  at the sublattice  $A$  ( $B$ ), and

$$M_{\mathbf{k}} = \begin{pmatrix} \varepsilon_{A,\mathbf{k}} - \mu & \varepsilon_{xy,\mathbf{k}} & \varepsilon_{T,\mathbf{k}} & 0 \\ \varepsilon_{xy,\mathbf{k}} & \varepsilon_{A,\mathbf{k}} - \mu & 0 & \varepsilon_{T,\mathbf{k}} \\ \varepsilon_{T,\mathbf{k}} & 0 & \varepsilon_{B,\mathbf{k}} - \mu & \varepsilon_{xy,\mathbf{k}} \\ 0 & \varepsilon_{T,\mathbf{k}} & \varepsilon_{xy,\mathbf{k}} & \varepsilon_{B,\mathbf{k}} - \mu \end{pmatrix}, \quad (3)$$

where

$$\begin{aligned} \varepsilon_{A,\mathbf{k}} &= -2(t_2 \cos k_x + t_3 \cos k_y), \\ \varepsilon_{B,\mathbf{k}} &= -2(t_2 \cos k_y + t_3 \cos k_x), \\ \varepsilon_{xy,\mathbf{k}} &= -2t_4(\cos k_x + \cos k_y), \\ \varepsilon_{T,\mathbf{k}} &= -4t_1 \cos \frac{k_x}{2} \cos \frac{k_y}{2}. \end{aligned} \quad (4)$$

$t_{1-4}$  are the hopping parameters and  $\mu$  is the chemical potential. Throughout the paper, the momentum  $\mathbf{k}$  is defined in the tetragonal notation.

The pairing term is

$$H_\Delta = \sum_{\mathbf{k}s\alpha} (\Delta_{\mathbf{k}} c_{s\alpha,\mathbf{k}\uparrow}^\dagger c_{s\alpha,-\mathbf{k}\downarrow}^\dagger + \text{H.c.}). \quad (5)$$

Here, we assume there exists only intraorbital pairing with extended  $s$ -wave pairing symmetry, and the SC order parameter is  $\Delta_{\mathbf{k}} = \frac{\Delta_0}{2}(\cos k_x + \cos k_y)$  similar to that obtained by spin fluctuations,<sup>18</sup> where

$$\Delta_0 = \frac{2V_{nmn}}{N} \sum_{\mathbf{k}} (\cos k_x + \cos k_y) \langle c_{s\alpha,-\mathbf{k}\downarrow} c_{s\alpha,\mathbf{k}\uparrow} \rangle \quad (6)$$

with  $V_{nmn}$  being a phenomenologically chosen next-nearest-neighbor attractive pairing interaction. It is well known that a similar nearest-neighbor density-density attraction of the form  $Vn_i n_{i+\delta}$  can lead to  $d$ -wave superconductivity in a mean-field treatment of the one-band repulsive  $U$  Hubbard model,<sup>36</sup> and here we merely generalize this concept to two orbitals and will show below this choice of  $V_{nmn}$  can lead to extended  $s$ -wave pairing in the two-orbital model. Here we need to point out that the origin of the attractive interaction is still unknown, it could originate from an effective attractive

density-density fluctuation dynamically generated in the original Hamiltonian or induced by particular phononic modes if an electron-phonon coupling is incorporated.<sup>37</sup> On the other hand, some theoretical works suggest that the pairing is mediated by exchanging spin fluctuations and conclude that the effective pairing interaction is repulsive in momentum space,<sup>18,38-40</sup> this is in contrast to our choice of momentum space interaction  $2V_{nmn}(\cos k_x + \cos k_y)$ , which can be attractive or repulsive depending on the momentum  $\mathbf{k}$ . So the pairing interaction in our model is different from that mediated by exchanging spin fluctuations. We also notice that in Ref. 41, the next-nearest-neighbor antiferromagnetic coupling  $J_2$  gives the same physics as our  $V_{nmn}$  when treated at the mean-field level and also can lead to extended  $s$ -wave pairing symmetry. Here we wish to emphasize that the purpose of the present paper is to study the interplay between the SDW and the extended  $s$ -wave SC, not the mechanism of superconductivity in this type of compound.

$H_{int}$  is the on-site interaction term which includes the Coulombic interaction and Hund coupling  $J_H$ , following Refs. 33 and 42, it can be expressed as

$$\begin{aligned} H_{int} &= U \sum_{ijs\alpha} n_{s\alpha,ij\uparrow} n_{s\alpha,ij\downarrow} + \left( U' - \frac{J_H}{2} \right) \sum_{ijs} n_{s0,ij} n_{s1,ij} \\ &\quad + J_H \sum_{ijs} (c_{s0,ij\uparrow}^\dagger c_{s0,ij\downarrow}^\dagger c_{s1,ij\downarrow} c_{s1,ij\uparrow} + \text{H.c.}) \\ &\quad - 2J_H \sum_{ijs} \mathbf{S}_{s0,ij} \cdot \mathbf{S}_{s1,ij}, \end{aligned} \quad (7)$$

where  $\{i, j\}$  denotes the unit cell,  $s=0$  ( $A$ ) or  $1$  ( $B$ ) is the sublattice index, and  $\alpha=0$  ( $d_{xz}$ ) or  $1$  ( $d_{yz}$ ) represents the orbital.  $n_{s\alpha,ij\sigma}$  and  $\mathbf{S}_{s\alpha,ij}$  are the density and spin operators in the orbital  $\alpha$  at the sublattice  $s$  of the unit cell  $\{i, j\}$ , respectively. According to symmetry, we have  $U' = U - 2J_H$ .<sup>42</sup> In the MF approach, we linearize  $H_{int}$  in momentum space as<sup>33,43</sup>

$$\begin{aligned} H_{int}^{\text{MF}} &= \frac{n}{4} (3U - 5J_H) \sum_{\mathbf{k}s\alpha\sigma} n_{s\alpha,\mathbf{k}\sigma} \\ &\quad - \frac{m}{2} (U + J_H) \sum_{\mathbf{k}s\alpha\sigma} \sigma c_{s\alpha,\mathbf{k}+\mathbf{Q}\sigma}^\dagger c_{s\alpha,\mathbf{k}\sigma}, \end{aligned} \quad (8)$$

where  $n=2+x$  is the number of electrons per lattice site and  $\mathbf{Q}=(\pi, \pi)$ . The SDW order parameter is

$$m = \frac{1}{N} \sum_{\mathbf{k}\sigma} \sigma \langle c_{s\alpha,\mathbf{k}+\mathbf{Q}\sigma}^\dagger c_{s\alpha,\mathbf{k}\sigma} \rangle \quad (9)$$

with  $N$  being the number of unit cells.

The effective MF Hamiltonian is then given by

$$H^{\text{MF}} = \sum_{\mathbf{k}} \varphi_{\mathbf{k}}^\dagger W_{\mathbf{k}} \varphi_{\mathbf{k}},$$

$$W_{\mathbf{k}} = \begin{pmatrix} M'_{\mathbf{k}} & R & \Delta_{\mathbf{k}}I & 0 \\ R & M'_{\mathbf{k}+\mathbf{Q}} & 0 & -\Delta_{\mathbf{k}}I \\ \Delta_{\mathbf{k}}I & 0 & -M'_{\mathbf{k}} & R \\ 0 & -\Delta_{\mathbf{k}}I & R & -M'_{\mathbf{k}+\mathbf{Q}} \end{pmatrix}, \quad (10)$$

where

$$\varphi_{\mathbf{k}}^{\dagger} = (\psi_{\mathbf{k}\uparrow}^{\dagger}, \psi_{\mathbf{k}+\mathbf{Q}\uparrow}^{\dagger}, \psi_{-\mathbf{k}\downarrow}, \psi_{-(\mathbf{k}+\mathbf{Q})\downarrow}),$$

$$M'_{\mathbf{k}} = M_{\mathbf{k}} + \frac{n}{4}(3U - 5J_H)I,$$

$$R = -\frac{m}{2}(U + J_H)I. \quad (11)$$

$I$  is a  $4 \times 4$  unit matrix and  $\Sigma'_{\mathbf{k}}$  means the summation extends over the magnetic Brillouin zone:  $-\pi < k_x \pm k_y \leq \pi$ . The MF Green's function matrix can be written as

$$g(\mathbf{k}, \tau) = -\langle T_{\tau} \varphi_{\mathbf{k}}(\tau) \varphi_{\mathbf{k}}^{\dagger}(0) \rangle \quad (12)$$

and

$$g(\mathbf{k}, ip_n) = A_{\mathbf{k}} W'_{\mathbf{k}} A_{\mathbf{k}}^{\dagger}, \quad (13)$$

where  $W'_{\mathbf{k}ij} = \delta_{ij}(ip_n - \lambda_{\mathbf{k}i})^{-1}$  and  $A_{\mathbf{k}}$  is a unitary matrix that satisfies  $(A_{\mathbf{k}}^{\dagger} W_{\mathbf{k}} A_{\mathbf{k}})_{ij} = \delta_{ij} \lambda_{\mathbf{k}i}$ .

The MF spin susceptibility is

$$\chi_{t\gamma, u\delta}^{r\alpha, s\beta(0)}(\mathbf{q}, \mathbf{q}', i\omega_n) = \frac{\delta_{\mathbf{q}', \mathbf{q}}}{2} \sum_{(i,j)=(p,o)}^{(o+8, p+8)} [P_{im, nj}(q) + P_{i+4m, nj+4}(q)], \quad (14)$$

here,  $r, s, t, u$  label the sublattice indices,  $\alpha, \beta, \gamma, \delta$  represent the orbitals, with

$$\begin{aligned} m &= 2r + \alpha + 1, \\ n &= 2s + \beta + 1, \\ o &= 2t + \gamma + 1, \\ p &= 2u + \delta + 1, \end{aligned} \quad (15)$$

and

$$P_{im, nj}(q) = -\frac{1}{\beta N} \sum_{\mathbf{k}} g_{im}(k) g_{nj}(k+q). \quad (16)$$

Here we use  $k=(\mathbf{k}, ip_n)$  and  $q=(\mathbf{q}, i\omega_n)$ .

We then use RPA to take into account the residual fluctuation of  $H_{int}$  beyond MF. The RPA spin susceptibility is determined by the matrix equation

$$\chi^{\text{RPA}}(q) = \sum_{r\alpha\gamma} \{ \chi^0(q) [I - \Gamma \chi^0(q)]^{-1} \}_{r\alpha, r\alpha}^{\gamma, \gamma}, \quad (17)$$

where  $I$  is a  $16 \times 16$  unit matrix and the nonzero elements of the interaction vertex are: for  $\alpha=\beta=\gamma=\delta$ ,  $\Gamma_{r\gamma, r\delta}^{\alpha, r\beta} = 2U$ ; for  $\alpha=\beta \neq \gamma=\delta$  or  $\alpha=\gamma \neq \beta=\delta$ ,  $\Gamma_{r\gamma, r\delta}^{\alpha, r\beta} = 2J_H$ .

The magnitudes of the parameters are chosen as  $t_{1-4} = 1, 0.4, -2, 0.04$ ,<sup>28</sup>  $U=3.4$ ,  $J_H=1.3$ ,  $V_{nmn} = -1.2$ ,<sup>33</sup> and the

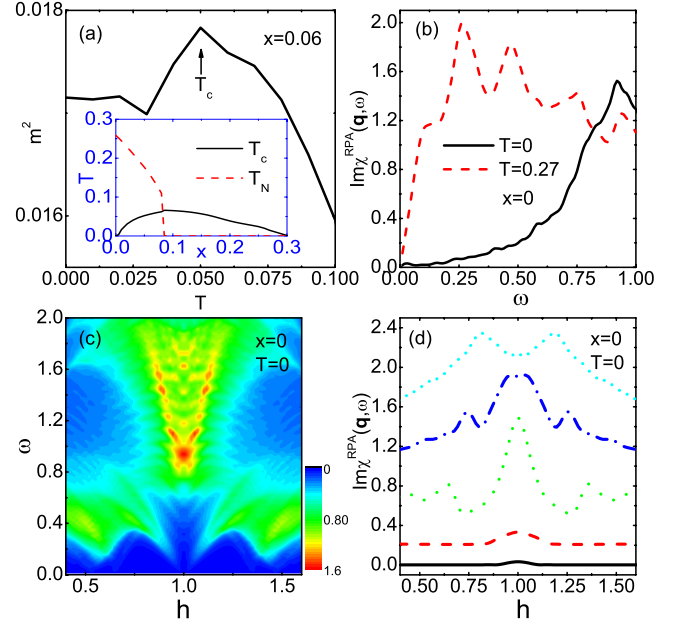


FIG. 1. (Color online) (a)  $m^2$  as a function of  $T$  close to  $T_c$  at  $x=0.06$ . Inset shows the calculated phase diagram. (b)  $\text{Im} \chi^{\text{RPA}}(\mathbf{q}, \omega)$  at  $\mathbf{q}=(\pi, \pi)$  as a function of  $\omega$  by changing  $i\omega_n$  to  $\omega+i\eta$ , at  $x=0$  and different temperatures  $T$ . (c)  $\text{Im} \chi^{\text{RPA}}(\mathbf{q}, \omega)$  as a function of energy transfer  $\omega$  and momentum  $\mathbf{q}$ , at  $x=0$  and  $T=0$ . The momentum is scanned along  $(q_x/\pi, q_y/\pi)=(h, h)$ . (d) Constant-energy scans along the  $(q_x/\pi, q_y/\pi)=(h, h)$  direction at  $x=0$  and  $T=0$ . Successive cuts are displaced vertically for clarity. The energy transfer is  $\omega=0.09$  (black solid),  $0.4$  (red dashed),  $0.93$  (green dotted),  $1.2$  (blue dashed dot), and  $2$  (cyan short dashed). The damping rate  $\eta=0.04$ .

number of unit cells is  $257 \times 257$ . Throughout the paper, the energies are measured in units of  $|t_1|$  and  $m$  is measured in units of Bohr magneton  $\mu_B$ . In order to enhance the numerical resolution as well as to show the pronounced effect of superconductivity on the spin dynamics, we artificially choose a large value of  $V_{nmn}$  which leads to a larger  $\Delta_0$  as compared to the experimental value. If we decrease the strength of  $V_{nmn}$  to half of its value, of course we can get a smaller  $\Delta_0$ , approximately five times smaller than its original value but such a small value will make the numerical calculation less accurate and more difficult to reach self-consistency.

### III. RESULTS AND DISCUSSION

First, we solve the MF equations self-consistently to obtain  $m$ ,  $\Delta_0$ , and  $\mu$  at different doping levels  $x$  and temperatures  $T$ . The calculated phase diagram as shown in the inset of [Fig. 1(a)] reproduces the result based on Bogoliubov-de Gennes equations<sup>33</sup> and is also qualitatively consistent with the experiments on  $\text{Ba}(\text{Fe}_{1-x}\text{Co}_x)_2\text{As}_2$ .<sup>4-6</sup> The difference between our paper and Ref. 33 around  $x=0.1$  is due to the size effect. Here we have a larger number of unit cells in momentum space self-consistent calculation and the initial values are always set to be random. We have carefully checked our calculation on systems with  $127 \times 127$ ,  $257 \times 257$ , and  $501$

$\times 501$  unit cells, respectively, and got the similar results. As a mean-field calculation, the values of  $T_c$  (Ref. 41) and  $T_N$  are often overestimated for two-dimensional systems. In most of other calculations (Ref. 44), the magnitudes of the SC and SDW order parameters were just put in by hand. Therefore, we could only compare our results with experiments qualitatively but not quantitatively. However, if we regard the SC order parameter and  $T_c$  obtained in our mean-field approximation correspond to the experimental values, then the comparison with experiments may become quantitative. Here the SDW and SC are competing with each other. If there is no SDW, SC would show up even in the parent compound. The presence of SC also suppresses SDW. For example, in the underdoped ( $x=0.06$ ) compound with  $T_N \approx 0.16$  and  $T_c \approx 0.05$ , the calculated magnitude of  $m^2$  (proportional to the magnetic Bragg-peak intensity) at  $T=0$  is reduced by  $\sim 4\%$  relative to that of the maximum intensity at  $T_c$  [see Fig. 1(a)], and this result is consistent with the neutron-diffraction experiments.<sup>4,8</sup> We also notice that our model gives  $m(T=0) \approx 0.22$  for the parent compound, which is smaller than the experimentally measured value  $\sim 0.9$ ,<sup>10</sup> suggesting that maybe more orbitals are needed in order to describe the parent compound.

Then, we investigate the spin dynamics in  $\text{Ba}(\text{Fe}_{1-x}\text{Co}_x)_2\text{As}_2$  for  $x=0, 0.06, 0.1$ , and  $0.2$ , corresponding to the undoped, underdoped, optimally doped and overdoped compounds, respectively.

In the parent ( $x=0$ ) compound, the RPA spin susceptibility [see Fig. 1(b)] in the paramagnetic state at  $T=0.27$  ( $T_N \approx 0.25$ ) shows a linear energy dependence for  $\omega < 0.1$ , suggesting gapless excitations.<sup>10,14</sup> On the other hand, in the SDW state at  $T=0$ , the spin excitation intensity is close to zero below  $\omega \approx 0.13$ , similar to a spin gap.<sup>9,10</sup> However, the gap is not sharp since a sharp gap would produce a stepwise increase in intensity at the gap energy which is unlike the more gradual increase seen here. Figures 1(c) and 1(d) show  $\text{Im} \chi^{\text{RPA}}(\mathbf{q}, \omega)$  as a function of energy transfer  $\omega$  and momentum  $\mathbf{q}$  along  $(q_x/\pi, q_y/\pi) = (h, h)$  direction at  $T=0$ . As we can see, there is almost no detectable intensity below  $\omega \approx 0.13$ , again illustrating the opening of the spin gap. The excitations are peaked at  $\mathbf{Q} = (\pi, \pi)$  and  $\omega \approx 0.93$ , at higher energies, the response is seen to split and broaden due to the dispersion of the spin waves. By tracking the peak positions in Fig. 1(c), the spin-wave dispersion relation can be fitted as  $\omega_q = \sqrt{\Delta^2 + v^2 q^2}$ ,<sup>10,15,45</sup> where  $\Delta \approx 0.93$  is an energy gap,  $v \approx 9.02$  is the spin-wave velocity, and  $q$  is the reduced wave vector away from  $(1,1)$  along the  $(h, h)$  direction. Here we need to make it clear that  $\omega \approx 0.13$  is a spin gap since below it, there is neither spin-flip particle-hole excitation nor collective spin-wave excitation. From  $\omega \approx 0.13$  to  $\omega \approx 0.93$ , there is spin-flip particle-hole excitation but no spin-wave excitation. Only above  $\omega \approx 0.93$ , there is collective spin-wave excitation and thus  $\Delta \approx 0.93$  is an energy gap in the spin-wave spectrum. Experimentally observed gap [7.7 or 9.8 meV, see the inset of Fig. 3 in Ref. 9 and Fig. 3(a) in Ref. 10] refers to the region, where there is neither spin-flip particle-hole excitation nor collective spin-wave excitation, corresponding to the  $\omega \approx 0.13$  case in our paper. The origin of the spin gap can be understood in terms of the Fermi surface at  $x=0$  as shown in Fig. 2(a) in Ref. 33. In the para-

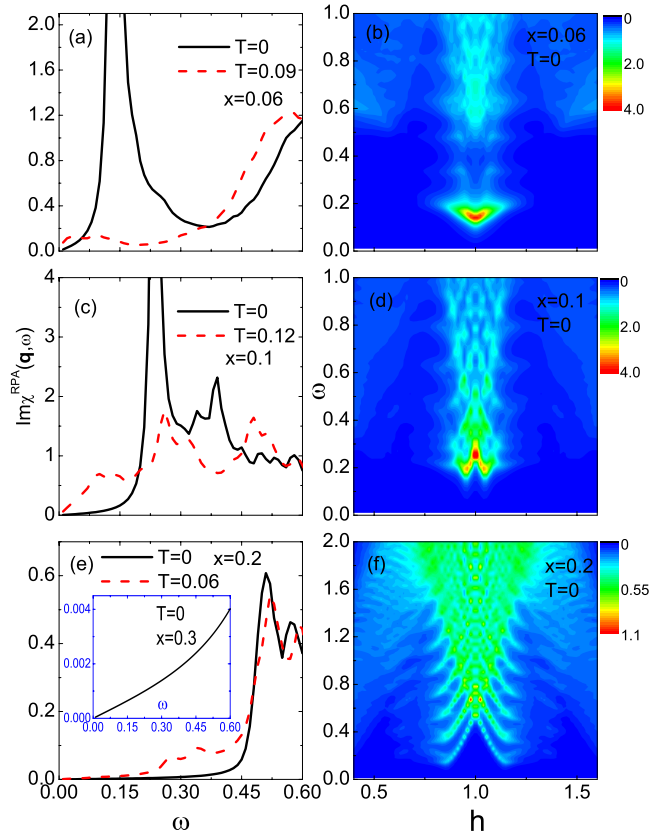


FIG. 2. (Color online) (a)  $\text{Im} \chi^{\text{RPA}}(\mathbf{q}, \omega)$  at  $\mathbf{q} = (\pi, \pi)$  as a function of  $\omega$ , at  $x=0.06$  and different temperatures  $T$ . (b)  $\text{Im} \chi^{\text{RPA}}(\mathbf{q}, \omega)$  as a function of energy transfer  $\omega$  and momentum  $\mathbf{q}$ , at  $x=0.06$  and  $T=0$ . The momentum is scanned along  $(q_x/\pi, q_y/\pi) = (h, h)$ . (c) and (d) [(e) and (f)] are similar to (a) and (b), respectively, but at  $x=0.1$  ( $x=0.2$ ). Inset in (e) shows the  $x=0.3$  case.

magnetic state, large parts of the two hole pockets around  $\Gamma = (0,0)$  and two electron pockets around  $M = (\pi, \pi)$  are nested by momentum  $(\pi, \pi)$ , thus giving rise to the gapless excitations at  $T=0.27$ . But at  $T=0$ , the SDW order will gap most parts of the original Fermi surface, leaving only tiny ungapped Fermi-surface pockets connected by  $(\pi, \pi)$  along the  $\Gamma$ - $M$  line, so in this case, for small energies, the imaginary part of the MF spin susceptibility is close to zero while its real part does not fulfill the resonance condition, leading to a spin-gap opening in the RPA spin susceptibility.

The RPA spin susceptibility [Fig. 2(a)] at  $x=0.06$  suggests that the excitations above  $T_c$  are gapless, although the intensity is very small at low energy. This may be the reason why above  $T_c$ , Ref. 4 claims the excitations are gapless while Ref. 8 concludes they are gapped. Below  $T_c$ , the intensities below  $\omega \approx 0.06$  and above  $\omega \approx 0.36$  are suppressed and the weight is transferred to form a resonance at  $\omega_{res} \approx 0.14$ . Since  $m(T=0.09) \approx 0.129$  and  $m(T=0) \approx 0.131$ , our results seem to agree with Ref. 4, which claims the resonance is produced by suppressing low-energy spectral weight, rather than Ref. 8, where the spectral weight is considered to be transferred from the ordered magnetic moments. In addition, Fig. 2(b) shows that below  $\omega_{res}$ , commensurate spin excitation prevails, in agreement with experimental observation,<sup>8</sup> and it becomes incommensurate when the energy is above  $\omega_{res}$ , no-

tably between  $\omega \approx 0.15$  and  $\omega \approx 0.18$ , which we predict to be measurable by NS experiment. The spin excitations can extend beyond  $\omega=1$  with smeared out and broadened features for  $\omega \geq 0.2$ .

At  $x=0.1$ , the SDW order is completely suppressed, and SC emerges for  $T < T_c \approx 0.06$ . The excitation spectrum [Fig. 2(c)] shows that in the superconducting state at  $T=0$ , a gap below  $\omega \approx 0.08$  develops and there is a resonance above the gap energy peaking at  $\omega_{res} \approx 0.24$ , qualitatively agrees with the NS experiments on the optimally doped  $\text{Ba}(\text{Fe}_{1-x}\text{Co}_x)_2\text{As}_2$ .<sup>11-14</sup> Furthermore, Fig. 2(d) shows that the spin excitation is incommensurate at low energy ( $0.18 \leq \omega \leq \omega_{res}$ ) which still need to be verified by experiments, then it switches to a commensurate behavior between  $\omega \approx \omega_{res}$  and  $\omega \approx 0.3$ , and becomes broad at higher energy, consistent with Refs. 12, 13, and 15. In the normal state at  $T=0.12$ , the spectrum is replaced by broad gapless excitations with a linear energy dependence for  $\omega < 0.1$ .<sup>13,14</sup> We notice a marked similarity between the spin excitations in the normal state of the optimally doped compound and those in the paramagnetic state of the parent compound as observed in Ref. 14, suggesting a common origin of spin fluctuations in both of them.

In contrast, the spin excitations in the overdoped ( $x=0.2$ ) compound [Fig. 2(e)] show gaplike behavior in both the normal and superconducting states. The origin of the gap may be due to one of the two hole pockets around  $\Gamma$  vanishes and the other one shrinks dramatically in the overdoped region according to ARPES experiments<sup>34</sup> and theories.<sup>28,33</sup> Under such a case, due to the lack of interband scattering between the hole and electron pockets, the imaginary part of the spin susceptibility is strongly suppressed and gives rise to the pseudogap behavior<sup>46</sup> which has been observed in NMR (Ref. 47) and NS (Ref. 14) experiments in the electron overdoped  $\text{Ba}(\text{Fe}_{1-x}\text{Co}_x)_2\text{As}_2$ . But in Ref. 46, the pseudogap is associated with the vanishing of one of three hole pockets around  $\Gamma$ , where experimentally there is only one hole pocket at this doping level as observed by ARPES.<sup>34</sup> The spin excitations in the superconducting state at  $T=0$  [Fig. 2(f)] are broader and weaker than those in the underdoped and optimally doped compounds, suggesting the importance of the hole pocket in enhancing the spin fluctuations.

At  $x=0.3$ , both the two hole pockets around  $\Gamma$  disappear,<sup>28,33</sup> our calculations show that SC is completely suppressed and the spin fluctuations are extremely small [the inset of Fig. 2(e)]. This further indicates the correlation between the electronic band structure and magnetism, and supports the scenario that the spin fluctuations in the underdoped regime, which serve as a precursor to SC, originate from quasiparticle scattering across the electron and hole pockets.

#### IV. CONCLUSION

In summary, we have systematically investigated the doping dependence of spin excitations in  $\text{Ba}(\text{Fe}_{1-x}\text{Co}_x)_2\text{As}_2$ ,

ranging from the parent to overdoped regime. In the parent compound, the spin excitations are gapless in the paramagnetic state and become strongly suppressed at low energy in the SDW state due to the opening of gaps on most parts of the original Fermi surface. For underdoped and optimally doped samples, the spin gaps and resonances at  $(\pi, \pi)$  only occur in the SC state. On the other hand, the spin excitations in the overdoped compound show gaplike behavior in both the normal and SC states due to the vanishing of one hole pocket around  $\Gamma$ , leading to a pseudogap behavior at this doping level. All the obtained results are in qualitative agreement with experiments. The changes in the spin dynamics at different doping levels may reflect changes in the electronic band structure and suggest a strong correlation between SC and magnetism.

Recently, optical conductivity measurements show a very large suppression of the Drude weight in  $\text{BaFe}_2\text{As}_2$ , to around 0.3 from the prediction of the band theory.<sup>48</sup> Whether RPA can account for such a small value of quasiparticle residue in the pnictides is still an open question. One of the authors has calculated this quantity in cuprates by using RPA and found that the suppression factor is from 0.06 to 0.42, depending on doping.<sup>49</sup> For the pnictides, so far there is no similar calculation based on RPA due to the complexity of multiband structure and indeed it needs a careful study. We also believe that the renormalization effect is possibly model dependant, which needs careful consideration. The dynamical mean-field theory is probably a more powerful method in studying the band renormalization effect<sup>50,51</sup> but it has not been applied to construct the phase diagram and the doping dependence of the spin excitations for the 122 family of iron pnictides, and its validity for the present problem still needs to be checked. In the present work, we mainly focus on the spin excitations, which are determined by the Fermi-surface nesting and evolution. In view of the agreement of the present calculations with experiments if we assume that the magnitudes of SC order parameter and  $T_c$  obtained from our mean-field calculation are comparable with those experimental values, the validity of RPA is qualitatively established. The optical conductivity which is different from the dynamic spin susceptibility is beyond the scope of the present study and it will constitute a subject for future investigation.

#### ACKNOWLEDGMENTS

We thank D. G. Zhang, C. H. Li, J. P. Hu, and J. X. Zhu for helpful discussions. This work was supported by the Texas Center for Superconductivity and the Robert A. Welch Foundation under Grants No. E-1070 (Y.G. and W.P.S.) and No. E-1146 (T.Z. and C.S.T.). T.Z. also acknowledges support from NSFC under Grant No. 11004105.

- <sup>1</sup>Y. Kamihara, T. Watanabe, M. Hirano, and H. Hosono, *J. Am. Chem. Soc.* **130**, 3296 (2008).
- <sup>2</sup>P. A. Lee, N. Nagaosa, and X.-G. Wen, *Rev. Mod. Phys.* **78**, 17 (2006), and references therein.
- <sup>3</sup>A. S. Sefat, R. Jin, M. A. McGuire, B. C. Sales, D. J. Singh, and D. Mandrus, *Phys. Rev. Lett.* **101**, 117004 (2008).
- <sup>4</sup>D. K. Pratt, W. Tian, A. Kreyssig, J. L. Zarestky, S. Nandi, N. Ni, S. L. Bud'ko, P. C. Canfield, A. I. Goldman, and R. J. McQueeney, *Phys. Rev. Lett.* **103**, 087001 (2009).
- <sup>5</sup>J. H. Chu, J. G. Analytis, C. Kucharczyk, and I. R. Fisher, *Phys. Rev. B* **79**, 014506 (2009); F. Ning, K. Ahilan, T. Imai, A. S. Sefat, R. Jin, M. A. McGuire, B. C. Sales, and D. Mandrus, *J. Phys. Soc. Jpn.* **78**, 013711 (2009).
- <sup>6</sup>C. Lester, J. H. Chu, J. G. Analytis, S. C. Capelli, A. S. Erickson, C. L. Condon, M. F. Toney, I. R. Fisher, and S. M. Hayden, *Phys. Rev. B* **79**, 144523 (2009).
- <sup>7</sup>M. Rotter, M. Tegel, and D. Johrendt, *Phys. Rev. Lett.* **101**, 107006 (2008); G. Wu, R. H. Liu, H. Chen, Y. J. Yan, T. Wu, Y. L. Xie, J. J. Ying, X. F. Wang, D. F. Fang, and X. H. Chen, *EPL* **84**, 27010 (2008); M. Rotter, M. Tegel, D. Johrendt, I. Schellenberg, W. Hermes, and R. Pottgen, *Phys. Rev. B* **78**, 020503(R) (2008).
- <sup>8</sup>A. D. Christianson, M. D. Lumsden, S. E. Nagler, G. J. MacDougall, M. A. McGuire, A. S. Sefat, R. Jin, B. C. Sales, and D. Mandrus, *Phys. Rev. Lett.* **103**, 087002 (2009).
- <sup>9</sup>R. A. Ewings, T. G. Perring, R. I. Bewley, T. Guidi, M. J. Pitcher, D. R. Parker, S. J. Clarke, and A. T. Boothroyd, *Phys. Rev. B* **78**, 220501(R) (2008).
- <sup>10</sup>K. Matan, R. Morinaga, K. Iida, and T. J. Sato, *Phys. Rev. B* **79**, 054526 (2009).
- <sup>11</sup>D. Parshall, K. A. Lokshin, J. Niedziela, A. D. Christianson, M. D. Lumsden, H. A. Mook, S. E. Nagler, M. A. McGuire, M. B. Stone, D. L. Abernathy, A. S. Sefat, B. C. Sales, D. G. Mandrus, and T. Egami, *Phys. Rev. B* **80**, 012502 (2009).
- <sup>12</sup>M. D. Lumsden, A. D. Christianson, D. Parshall, M. B. Stone, S. E. Nagler, G. J. MacDougall, H. A. Mook, K. Lokshin, T. Egami, D. L. Abernathy, E. A. Goremychkin, R. Osborn, M. A. McGuire, A. S. Sefat, R. Jin, B. C. Sales, and D. Mandrus, *Phys. Rev. Lett.* **102**, 107005 (2009).
- <sup>13</sup>D. S. Inosov, J. T. Park, P. Bourges, D. L. Sun, Y. Sidis, A. Schneidewind, K. Hradil, D. Haug, C. T. Lin, B. Keimer, and V. Hinkov, *Nat. Phys.* **6**, 178 (2010).
- <sup>14</sup>K. Matan, S. Ibuka, R. Morinaga, S. Chi, J. Lynn, A. Christianson, M. Lumsden, and T. Sato, *Phys. Rev. B* **82**, 054515 (2010).
- <sup>15</sup>C. Lester, J. H. Chu, J. G. Analytis, T. G. Perring, I. R. Fisher, and S. M. Hayden, *Phys. Rev. B* **81**, 064505 (2010).
- <sup>16</sup>W. Lv, F. Krüger, and P. Phillips, *Phys. Rev. B* **82**, 045125 (2010).
- <sup>17</sup>M. A. Kastner and R. J. Birgeneau, *Rev. Mod. Phys.* **70**, 897 (1998).
- <sup>18</sup>I. I. Mazin, D. J. Singh, M. D. Johannes, and M. H. Du, *Phys. Rev. Lett.* **101**, 057003 (2008).
- <sup>19</sup>M. M. Korshunov and I. Eremin, *Phys. Rev. B* **78**, 140509 (2008); T. A. Maier and D. J. Scalapino, *ibid.* **78**, 020514(R) (2008).
- <sup>20</sup>J. Knolle, I. Eremin, A. V. Chubukov, and R. Moessner, *Phys. Rev. B* **81**, 140506(R) (2010).
- <sup>21</sup>M. M. Korshunov and I. Eremin, *EPL* **83**, 67003 (2008).
- <sup>22</sup>C. Liu, G. D. Samolyuk, Y. Lee, N. Ni, T. Kondo, A. F. Santander-Syro, S. L. Bud'ko, J. L. McChesney, E. Rotenberg, T. Valla, A. V. Fedorov, P. C. Canfield, B. N. Harmon, and A. Kaminski, *Phys. Rev. Lett.* **101**, 177005 (2008); K. Nakayama, T. Sato, P. Richard, Y.-M. Xu, Y. Sekiba, S. Souma, G. F. Chen, J. L. Luo, N. L. Wang, H. Ding, and T. Takahashi, *EPL* **85**, 67002 (2009); D. V. Evtushinsky, D. S. Inosov, V. B. Zabolotnyy, A. Koitzsch, M. Knupfer, B. Büchner, M. S. Viazovska, G. L. Sun, V. Hinkov, A. V. Boris, C. T. Lin, B. Keimer, A. Varykhalov, A. A. Kordyuk, and S. V. Borisenko, *Phys. Rev. B* **79**, 054517 (2009); K. Hashimoto, T. Shibauchi, T. Kato, K. Ikada, R. Okazaki, H. Shishido, M. Ishikado, H. Kito, A. Iyo, H. Eisaki, S. Shimoto, and Y. Matsuda, *Phys. Rev. Lett.* **102**, 017002 (2009).
- <sup>23</sup>H. Ding, P. Richard, K. Nakayama, K. Sugawara, T. Arakane, Y. Sekiba, A. Takayama, S. Souma, T. Sato, T. Takahashi, Z. Wang, X. Dai, Z. Fang, G. F. Chen, J. L. Luo, and N. L. Wang, *EPL* **83**, 47001 (2008); X. G. Luo, M. A. Tanatar, J.-Ph. Reid, H. Shakeripour, N. Doiron-Leyraud, N. Ni, S. L. Bud'ko, P. C. Canfield, H. Luo, Z. Wang, H.-H. Wen, R. Prozorov, and L. Taillefer, *Phys. Rev. B* **80**, 140503(R) (2009); R. T. Gordon, N. Ni, C. Martin, M. A. Tanatar, M. D. Vannette, H. Kim, G. D. Samolyuk, J. Schmalian, S. Nandi, A. Kreyssig, A. I. Goldman, J. Q. Yan, S. L. Bud'ko, P. C. Canfield, and R. Prozorov, *Phys. Rev. Lett.* **102**, 127004 (2009).
- <sup>24</sup>H.-J. Grafe, D. Paar, G. Lang, N. J. Curro, G. Behr, J. Werner, J. Hamann-Borrero, C. Hess, N. Leps, R. Klingeler, and B. Büchner, *Phys. Rev. Lett.* **101**, 047003 (2008).
- <sup>25</sup>J. D. Fletcher, A. Serafin, L. Malone, J. G. Analytis, J.-H. Chu, A. S. Erickson, I. R. Fisher, and A. Carrington, *Phys. Rev. Lett.* **102**, 147001 (2009); C. W. Hicks, T. M. Lippman, M. E. Huber, J. G. Analytis, J.-H. Chu, A. S. Erickson, I. R. Fisher, and K. A. Moler, *ibid.* **103**, 127003 (2009).
- <sup>26</sup>Y. Nakai, T. Iye, S. Kitagawa, K. Ishida, S. Kasahara, T. Shibauchi, Y. Matsuda, and T. Terashima, *Phys. Rev. B* **81**, 020503(R) (2010).
- <sup>27</sup>Z.-J. Yao, J.-X. Li, and Z. D. Wang, *New J. Phys.* **11**, 025009 (2009); F. Wang, H. Zhai, Y. Ran, A. Vishwanath, and D.-H. Lee, *Phys. Rev. Lett.* **102**, 047005 (2009).
- <sup>28</sup>D. Zhang, *Phys. Rev. Lett.* **103**, 186402 (2009).
- <sup>29</sup>M. Daghofer and A. Moreo, *Phys. Rev. Lett.* **104**, 089701 (2010).
- <sup>30</sup>D. Zhang, *Phys. Rev. Lett.* **104**, 089702 (2010).
- <sup>31</sup>S. Raghu, X.-L. Qi, C.-X. Liu, D. J. Scalapino, and S.-C. Zhang, *Phys. Rev. B* **77**, 220503(R) (2008).
- <sup>32</sup>M. Daghofer, A. Moreo, J. A. Riera, E. Arrigoni, D. J. Scalapino, and E. Dagotto, *Phys. Rev. Lett.* **101**, 237004 (2008).
- <sup>33</sup>T. Zhou, D. Zhang, and C. S. Ting, *Phys. Rev. B* **81**, 052506 (2010).
- <sup>34</sup>K. Terashima, Y. Sekiba, J. H. Bowen, K. Nakayama, T. Kawahara, T. Sato, P. Richard, Y.-M. Xu, L. J. Li, G. H. Cao, Z.-A. Xu, H. Ding, and T. Takahashi, *Proc. Natl. Acad. Sci. U.S.A.* **106**, 7330 (2009); Y. Sekiba, T. Sato, K. Nakayama, K. Terashima, P. Richard, J. H. Bowen, H. Ding, Y.-M. Xu, L. J. Li, G. H. Cao, Z.-A. Xu, and T. Takahashi, *New J. Phys.* **11**, 025020 (2009).
- <sup>35</sup>S. H. Pan, A. Li, and J. H. Ma (private communication).
- <sup>36</sup>E. Dagotto, J. Riera, Y. C. Chen, A. Moreo, A. Nazarenko, F. Alcaraz, and F. Ortolani, *Phys. Rev. B* **49**, 3548 (1994); A. Nazarenko, A. Moreo, E. Dagotto, and J. Riera, *ibid.* **54**, R768 (1996), and references therein.
- <sup>37</sup>A. Moreo, M. Daghofer, J. A. Riera, and E. Dagotto, *Phys. Rev.*

- B 79**, 134502 (2009).
- <sup>38</sup>S. Graser, T. A. Maier, P. J. Hirschfeld, and D. J. Scalapino, *New J. Phys.* **11**, 025016 (2009).
- <sup>39</sup>A. V. Chubukov, D. V. Efremov, and I. Eremin, *Phys. Rev. B* **78**, 134512 (2008).
- <sup>40</sup>A. V. Chubukov, M. G. Vavilov, and A. B. Vorontsov, *Phys. Rev. B* **80**, 140515(R) (2009).
- <sup>41</sup>K. Seo, B. A. Bernevig, and J. Hu, *Phys. Rev. Lett.* **101**, 206404 (2008).
- <sup>42</sup>A. M. Oleś, G. Khaliullin, P. Horsch, and L. F. Feiner, *Phys. Rev. B* **72**, 214431 (2005).
- <sup>43</sup>Z. Y. Weng, T. K. Lee, and C. S. Ting, *Phys. Rev. B* **38**, 6561 (1988); J. R. Schrieffer, X. G. Wen, and S. C. Zhang, *ibid.* **39**, 11663 (1989).
- <sup>44</sup>M. M. Parish, J. Hu, and B. A. Bernevig, *Phys. Rev. B* **78**, 144514 (2008); K. Seo, C. Fang, B. A. Bernevig, and J. Hu, *ibid.* **79**, 235207 (2009); A. Moreo, M. Daghofer, A. Nicholson, and E. Dagotto, *ibid.* **80**, 104507 (2009).
- <sup>45</sup>R. J. McQueeney, S. O. Diallo, V. P. Antropov, G. D. Samolyuk, C. Broholm, N. Ni, S. Nandi, M. Yethiraj, J. L. Zarestky, J. J. Pulikkotil, A. Kreyssig, M. D. Lumsden, B. N. Harmon, P. C. Canfield, and A. I. Goldman, *Phys. Rev. Lett.* **101**, 227205 (2008); S. O. Diallo, V. P. Antropov, T. G. Perring, C. Broholm, J. J. Pulikkotil, N. Ni, S. L. Bud'ko, P. C. Canfield, A. Kreyssig, A. I. Goldman, and R. J. McQueeney, *ibid.* **102**, 187206 (2009).
- <sup>46</sup>H. Ikeda, R. Arita, and J. Kuneš, *Phys. Rev. B* **82**, 024508 (2010).
- <sup>47</sup>F. L. Ning, K. Ahilan, T. Imai, A. S. Sefat, M. A. McGuire, B. C. Sales, D. Mandrus, P. Cheng, B. Shen, and H.-H. Wen, *Phys. Rev. Lett.* **104**, 037001 (2010).
- <sup>48</sup>M. M. Qazilbash, J. J. Hamlin, R. E. Baumbach, L. Zhang, D. J. Singh, M. B. Maple, and D. N. Basov, *Nat. Phys.* **5**, 647 (2009).
- <sup>49</sup>J.-X. Li, T. Zhou, and Z. D. Wang, *Phys. Rev. B* **72**, 094515 (2005).
- <sup>50</sup>K. Haule, J. H. Shim, and G. Kotliar, *Phys. Rev. Lett.* **100**, 226402 (2008).
- <sup>51</sup>M. Aichhorn, L. Pourovskii, V. Vildosola, M. Ferrero, O. Parcollet, T. Miyake, A. Georges, and S. Biermann, *Phys. Rev. B* **80**, 085101 (2009).